ICES2006-1411

Modeling of Variable Intake Valve Timing in SI Engine

S. Ahmad Ghazi Mir Saied
Faculty of Mech. Eng.
K.N.Toosi University of Technology
Tehran, IRAN

S.Ali Jazayeri
Faculty of Mech. Eng.
K.N.Toosi University of Technology
Tehran, IRAN

Amir H. Shamekhi
Faculty of Mech. Eng.
K.N.Toosi University of Technology
Tehran, IRAN

ABSTRACT

In internal combustion engines valve events and timings are among the most important parameters which have a major influence on the engine's operation and volumetric efficiency. By using camless valvetrain strategy, improvement in fuel economy as well as an increase in entering air charge is found throughout the engine map with the largest benefits arising from low speed operating conditions. The system offers a continuously variable and independent control of virtually all parameters of valve motion. This permits optimization of valve events for each operating condition without any compromise.

In this paper we describe a phenomenological model for an unthrottled operation of a camless intake process of spark-ignited (SI) engine. Initially the cylinder breathing dynamics is modeled and results are validated with experimental data of a conventional engine with cam-driven valve profile during unthrottled operation. Then we determine the most optimized intake valve profile in order to have the most volumetric efficiency and proper operation for each operating condition based on the existing model and using numerical techniques.

KEY WORDS: optimization, SI engine, variable valve timing, volumetric efficiency.

INTRODUCTION

Most of today's piston-type internal combustion engines use mechanically driven camshafts to operate the intake and exhaust valves. Such conventional mechanical valvetrains generally use valve timings and lifts that are fixed depending upon their design. The fixed-valve events of conventional cam-controlled engines compromise the engine for better performance under all operating conditions. The lack of flexibility of camshaft-based valvetrains to vary timing, duration and lift of intake valves, is one of the disadvantages of conventional SI engines. The valve timings and lifts that are optimal for an engine's top-end performance, high lifts, are different from those required for fuel economy at part load. If the intake and exhaust valve events are designed to achieve high volumetric efficiency or power at high engine speeds which is the case in most engine designs, engine operation would severely hampered at low speeds and loads. Therefore, the valve events of a variable valvetrain system that vary with speed and load anywhere on the engine map would achieve high volumetric efficiency (power) at high speeds, while also satisfying demands for low fuel consumption and high volumetric efficiency under part load operation.

One way to improve the most important performance characteristics of SI engines such as fuel economy and volumetric efficiency is to run with wide open throttle at all speed/load conditions, and to control the cylinder intake air flow by optimizing the motion of the intake valves by means of electrohydraulic camless valvetrain. The inlet valve timing is the most important parameter for optimizing the engine volumetric efficiency.

Some studies have shown that variable intake valve timing cause major reduction in pumping losses and fuel consumption (Ma [1], Gray [2], and Elrod [3]). Work in the area of maximum lift control that enables stable actuator operation for the electro-hydraulic camless valvetrain can be found in Anderson [4] and Kim [5]. There are useful discussions for electrically actuated valves in [6] and [7]. Engine sensitivity analysis and optimization issues can be found in Ahmad [8], Sono [9], For selectively optimizing the valve timing, lift, event duration, and other parameters of the valve motion for each operating condition, a system offering a total valve motion control is needed. Elecetrohydraulic camless valvetrain brings about a system that allows independent scheduling of valve lift, valve open duration, and placement of the event in the engine

cycle, thus creating an engine with a totally uncompromised operation. This is a significant advancement over the conventional mechanical valvetrain. Freedom to optimize all parameters of valve motion for each engine operating condition without compromise is expected to result in better fuel economy, higher volumetric efficiency and a number of other benefits and possibilities [10].

Unique to infinite lift control is the ability to use the intake valve to control the throttling of the engine. This is achieved by eliminating the need to throttle the air flow into the intake manifold which is the traditional means of controlling the engine load in spark ignition engines. Without a throttle valve, control of the air flow into the cylinders can be realized by adjusting the effective area of the intake valves and by variation of the intake valve opening period. We refer to this engine conditions as unthrottled operation.

Initially, mathematical formulation of each engine subsystem is presented. We modify a phenomenological multicylinder and crankangle based model of the intake process presented by Stefanopoulou, A.G. [11] and moraal et al. [12]. The model is validated with experimental data of a conventional engine using cam-driven valve profile during unthrottled operation.

This paper is concerned only with the induction process of engine cycle. The model that is developed in the following section is based on a plenum model to the extent that the pressures in the intake manifold and cylinders are assumed to be uniform. Pressure at the intake valve between the manifold and the cylinder is assumed to be equal to the intake manifold pressure and terms describing pressure fluctuation due to acoustic and inertial effects at the inlet port will be neglected. [13]

NOMENCLATURE

IVD : intake valve duration

IVL : intake valve maximum lift

IVO : intake valve opening

IVP : intake valve profile

$\dot{m}_c$: mass air flow rate through the intake port

$\dot{m}_\phi$: mass air flow rate through the throttle

N : engine speed (RPM)

$p_\circ$: ambient pressure (=1 bar)

p_c : cylinder pressure

p_m : intake manifold pressure

R : specific gas constant (=287 J/kg.K)

T : air temperature

V_c : cylinder volume

V_{cyl} : cylinder clearance volume

V_d : cylinder displaced volume

V_m : intake manifold volume

ϕ : throttle angle

θ : crank angle

$s_r, s_c, s_s, d_s, and\ \lambda$: intake valve profile parameters

η_v : volumetric efficiency

ENGINE MODEL

In this section, we describe a dynamic, phenomenological model of the induction process in multi-cylinder engine that is based on mean value approximation of the engine states after averaging over an engine event. The model is low-frequency, nonlinear and continuous in time and use a lumped parameter approximation of breathing dynamics. The model contains parameters which we need for optimization such as intake valve lift profile and engine speed.

THROTTLE BODY

A quasi-steady model of flow through an orifice is used to derive the mass air flow through the throttle body and the intake valve. The basic throttle body model assumes one-dimensional, steady, compressible flow of an ideal gas. The mass air flow into the manifold, $\dot{m}_\phi$, is approximated as a function of the throttle effective flow area $A(\phi)$, upstream pressure ($p_\circ$) and the downstream pressure, which is manifold pressure (p_m). Upstream pressure is assumed to be atmospheric (i.e. $p_\circ$ =100 kPa):

$$\dot{m}_\phi = A_\phi(\phi)d(p_m, p_o) \qquad (1)$$

Where for the particular engine modeled:

$$A_\phi = 1.268\times10^{-4}\left(-0.2215 - 2.275\phi + 0.23\phi^2\right) \qquad (2)$$

And

$$d(p_m, p_o) = \begin{cases} 1 & \frac{p_m}{p_\circ} < 0.5 \\ 2\sqrt{\frac{p_m}{p_o} - \left(\frac{p_m}{p_o}\right)^2} & if \quad 0.5 \le \frac{p_m}{p_\circ} < 1 \\ -d(p_o, p_m) & \frac{p_m}{p_\circ} > 1 \end{cases} \qquad (3)$$

INTAKE MANIFOLD DYNAMICS

The intake manifold and cylinders can be represented as finite volumes based on the "Filling and Emptying Methods" of plenum modeling described in [14].

The dynamic relationship for the mass flow rate of air out of the intake manifold was developed by employing the principles of conservation of mass and energy, and the equation of state for an ideal gas. Homogenous temperature and pressure are assumed and differences in intake flow temperature and manifold temperature can be neglected for the intake event.

The state equation is given as:

$$\frac{dp_m}{dt} = \frac{RT}{V_m}\left[\dot{m}_\phi - \sum_{i=1}^{n} \dot{m}_{c_i}\right] \qquad (4)$$

Where, $\dot{m}_\phi$ is the mass air flow through the throttle (kg/s), $\dot{m}_{ci}$ is the mass air flow from the manifold into cylinder i (kg/s), p_m is the intake manifold pressure, $R = 287 \frac{J}{kg.K}$ is the specific gas constant, $T = 293K$ is the nominal manifold temperature, $V_m = 0.001m^3$ is the manifold volume, $i = 1, \dots, n,$ where the subscript i denotes the ith cylinder and n is the number of the cylinders.

CYLINDER BREATHING DYNAMICS

Exactly same as intake manifold dynamics, the dynamic equations that describe the breathing process are based on the principles of conservation of mass and ideal gas law. The state equation is given as:

$$\frac{dp_{c_i}}{dt} = \frac{1}{V}\left[RT\dot{m}_{c_i} - \dot{V}_{c_i}p_{c_i}\right], \quad i = 1, \dots, n, \qquad (5)$$

Where, p_{c_i} is the cylinders pressure, and V_{c_i} is the ith cylinder volume (m^3).

The cylinder volume is a function of the crankangle (θ) in degrees [14]:

$$V_{c_i}(\theta) = \frac{V_d}{2}\left(1 - \cos\left(\theta - \frac{720}{n}(i-1)\right)\right) + V_{cl}, \qquad (6)$$

$$\theta = \left(\int_0^t \frac{N}{60} 360.dt\right) \bmod 720^\circ, \qquad (7)$$

Where, V_d is the maximum cylinder displaced volume, V_{cl} is the cylinder clearance volume, and N is the engine speed (rpm).

The mass air flow from the manifold into the cylinder will be stated as follows:

$$\dot{m}_{c_i} = A_{v_i}\left(L_{v_i}\right)d\left(p_{c_i}, p_m\right) \qquad (8)$$

Where

$$d\left(p_{c_i}, p_m\right) = \begin{cases} 1 & \frac{p_{c_i}}{p_m} < 0.5 \\ 2\sqrt{\frac{p_{c_i}}{p_m} - \left(\frac{p_{c_i}}{p_m}\right)^2} & if \quad 0.5 \le \frac{p_{c_i}}{p_m} < 1 \\ -d\left(p_m, p_{c_i}\right) & \frac{p_{c_i}}{p_m} > 1 \end{cases} \qquad (9)$$

and $A_v(L_v)$ is the valve effective flow area that is described in the following section.

VALVE EFFECTIVE FLOW AREA

Lift equation describes the geometric flow characteristics across the intake valve for each cylinder as a function of crankangle θ, scaled by the characteristics air charge coefficient α.

The intake valve profile motion, IVP, is controlled by the valve opening, IVO in degrees, the maximum valve lift, IVL in mm, and the valve duration, IVD in degrees [10].

We can approximate the scaled effective valve flow area as a linear function of the lift

$$A_v(L_{v_i}) = \alpha L_v \tag{10}$$

The scale factor α is identified as 0.0175 in reference [14] for the experimental engine under consideration.

The models for intake valve lift profile can be categorized as two types: Conventional valve lift model and camless valve lift model.

CONVENTIONAL VALVE LIFT

The conventional valve lift motion is characterized by open timing instant (IVO), maximum lift (IVL), and open duration period (IVD). For a conventional engine, the valve lift is a sinusoidal function of these parameters and crank angle during an intake event:

$$L_v(u_t, u_l, u_d, \theta) = u_l \cdot \sin^2\left(\frac{180}{u_d}(\theta - u_t)\right) \tag{11}$$

The Conventional intake valve profile is shown in Fig. 1. The expression given for the valve lift implies that there is no overlap of individual intake lift profiles. Although this is not true for conventional valve trains, it have been seen that this simplification has hardly any effect on the model accuracy [12].

CAMLESS VALVE LIFT

We can characterize the camless valve motion by timing (or opening) IVO, maximum lift IVL, and duration IVD of each intake valve. For simplicity, we model the intake valve profiles with a smooth exponential opening. The variables IVO, IVL, and IVD are chosen to achieve the demanded cylinder air charge. The camless intake valve lift profile model presented in this paper is a modified version of model described in [15] which causes significant improvement in consistency of this sub-model.

$$L_v(IVO, IVL, IVD, t)$$
$$= \begin{cases} s_r(t - t_1) & t_1 \leq t < t_2 \\ IVL - L_s \exp\left(-\frac{s_r}{L_s}(t - t_2)\right) & t_2 \leq t < t_3 \\ IVL - L_s \exp\left(-\frac{s_r}{L_s}\left(\frac{s}{2} - (t - t_3)\right)\right) & t_3 \leq t < t_4 \\ -s_r(t - t_4) + (1 - \lambda)IVL & t_4 \leq t < t_5 \\ s_s(t - t_5) - s_s d_s & t_5 \leq t < t_6 \\ 0 & otherwise \end{cases} \tag{12}$$

Where
$$t_1 = t_{IVO}, t_2 = t_{IVO} + d_r, t_3 = t_{IVO} + d_r + s/2$$
$$t_4 = t_{IVO} + d_r + s, t_5 = t_{IVO} + t_{IVD} - d_s,$$
$$t_6 = t_{IVO} + t_{IVD}, \ d_r = (1 - \lambda) \cdot IVL/s_r,$$
$$d_f = ((1 - \lambda) \cdot IVL + s_s d_s)/s_r, \ L_s = \lambda \cdot IVL,$$
$$s = t_{IVD} - (d_r + d_f + d_s)$$
and

t_{IVO} : Opening time of intake valve opening

t_{IVD} : Duration of intake valve opening

s_r : Intake valve opening inclination

s_c : Intake valve closing inclination

s_s : Inclination of intake valve seating

d_s : Duration of intake valve seating

λ : Parameter determining how fast the valve motion approaches the maximum lift after opening instant

The constants s_r, s_c, s_s, and d_s are fixed in the time domain. A coordinate transformation to crankangle domain results in different valve profiles for different engine speeds.

The area defined by the intake valve profile, IVP, is significantly reduced at higher engine speeds as shown in Fig. 2.

VOLUMETRIC EFFICIENCY

Volumetric efficiency (η_v) is a measure that how effective an engine is freshly charged [14]:

$$\eta_v = \frac{2\dot{m}_a}{\rho_{a,i}V_d N} \qquad (13)$$

Where $\rho_{a,i}$ is the inlet air density. An alternative equivalent definition for volumetric efficiency is:

$$\eta_v = \frac{m_a}{\rho_{a,i}V_d} \qquad (14)$$

Where m_a is the mass of air inducted into the cylinder per cycle.

In this work, air inlet density and air intake manifold are taken to be the same (in this case η_v measures the pumping performance of the inlet port and valve only). It is shown that the most important parameters affecting the volumetric efficiency are intake valve lift, and timing [14].

SIMULATION RESULTS

The nonlinear and coupled differential equations of the above-mentioned model were coded in Matlab Simulink software. To initialize the simulation, the manifold pressure is assumed to be equal to the ambient pressure, $p_m(0) = p_\circ$ since the throttle is wide open and the cylinder pressure is assumed to be equal to the exhaust backpressure, $p_{ci}(IVO) = 1.1bar$ since the model does not take into account the overlap between the intake and exhaust valves and describes only the intake event of the engine cycle.

Figures 3, 4, and 5 show the simulation results. For intake valve profile shown in Fig.3, the pressure p_m, and p_{c_i} are plotted against the crank angle in Fig. 4, and the mass air flow rates $\dot{m}_\phi$ and $\dot{m}_{ci}$ are plotted against the crank angle in Fig. 5. For the values that has been used in this simulation, the intake valve opening (IVO) is equal to 0 deg, lift is equal to 3 mm, closing timing is equal to 180 deg and since the intake valve duration IVD is equal to the closing timing plus the seating duration, IVD is equal to 189 deg. As can be seen in Fig. 5, the air mass flow rate to manifold and cylinder are very similar because the rate of change of the manifold pressure is small.

The manifold pressure, p_m stays close to the ambient pressure due to unthrottled operation.

When the intake valve opens, the mass air flow is negative (backflow through the intake valves), because the cylinder pressure is higher than the manifold pressure. The downward piston motion causes the cylinder pressure, p_{ci} to drop from its initial value and consequently causes the air to flow from the manifold to the cylinder for the rest of the intake valve duration.

Fig. 6 shows the simulation results for volumetric efficiency sub-model. The values that have been used for this model simulation are the same as the values that have been used for breathing process model simulation.

MODEL VALIDATION

For the validation of the breathing process simulation results that obtained in previous section, we compare the results of an above-mentioned engine model including conventional intake profile for wide open throttle condition (i.e. ϕ in Eq. [1] is fixed to 90 deg) with experimental data for a 4-cylinder engine [12] at engine speeds of 1500 and 3000 rpm. The valves of the experimental engine are cam-driven, therefore, the intake valve profile is the conventional sinusoidal profile.

For the validation of the volumetric efficiency simulation results that obtained in previous section, we compare the results of volumetric efficiency sub-model with experimental data for an engine with specifications described in [16] in Fig. 11. As it can be seen in Fig. 11 the most deviation of simulation results from experimental values is 7.5 percent.

OPTIMIZATION

In this section we perform numerical optimization in order to postulate optimal valve geometry and timing for maximizing volumetric efficiency in terms of the camless intake valve lift profile, inlet valve opening, and optimal inlet valve closing timing. Because the intake valve lift profile and its timing affect the amount of entering charge, they thus affect the volumetric efficiency. In following section we present the optimization strategy for the camless intake valve lift profile.

In optimization problems the objective is to determine a function that maximizes a specified functional (Cost function).

An optimization process formulation includes three steps as follows:

1. Definition of a mathematical model

2. Determination of a performance criterion
3. Demonstrating the constraints.

PROBLEM FORMULATION

We have described the first step in previous sections. We are faced with the problem of selecting functions x_1, x_2, x_3 on the interval $[t_\circ, t_f]$ to maximize the cost functional

$$J(x_1, x_2, x_3) = \int_{t_\circ}^{t_f} g(x_1(t), x_2(t), x_3(t), \dot{x}_1(t), \dot{x}_2(t), \dot{x}_3(t), t) dt \quad (15)$$

It is much more convenient and compact to use matrix notation. Therefore, for the problem statement, we have

$$\mathbf{J}(\mathbf{X}) = \int_{t_o}^{t_f} \mathbf{g}(\mathbf{x}(t), \dot{\mathbf{x}}(t), t) dt \quad (16)$$

The cost function presented in Eq. (16) is called the Lagrange form. Necessary condition for x to be an extremal is the matrix representation of the Euler equations:

$$\frac{\partial \mathbf{g}}{\partial \mathbf{x}}(\mathbf{x}^*(t), \dot{\mathbf{x}}^*(t), t) - \frac{d}{dt}\left[\frac{\partial \mathbf{g}}{\partial \dot{\mathbf{x}}}(\mathbf{x}^*(t), \dot{\mathbf{x}}^*(t), t)\right] = 0 \quad (17)$$

(Euler Equation)

And the boundary conditions:
$$\mathbf{x}(t_\circ) = \mathbf{x}_\circ,$$
$$\mathbf{x}(t_f) = \mathbf{x}_f$$
Where

$$\mathbf{x}(t) = \begin{bmatrix} x_1(t) \\ x_2(t) \\ x_3(t) \end{bmatrix} \quad and \quad \dot{\mathbf{x}}(t) = \begin{bmatrix} \dfrac{d}{dt}x_1(t) \\ \dfrac{d}{dt}x_2(t) \\ \dfrac{d}{dt}x_3(t) \end{bmatrix}$$

Thus we arrive at the two-point boundary value problem $(TPBVP)$. Usually, $TPBVP$ is nonlinear problem that cannot be solved analytically to obtain the optimal function x, thus we use an iterative numerical technique for determining optimal function x called variation of extremals.

In many physical problems of interest there are various inequality constraints on the input vector. When inequality constraints are present it is necessary that we consider them in determining optimum system design. Thus we are faced with maximizing a cost function of the form

$$\mathbf{J}(\mathbf{X}) = \int_{t_\circ}^{t_f} \mathbf{g}(\mathbf{x}(t), \dot{\mathbf{x}}(t), t) dt \quad (18)$$

And inequality constraint of the form

$$\Gamma_{min} \le \Gamma(\mathbf{x}, \dot{\mathbf{x}}, t) \le \Gamma_{max} \quad (19)$$

The technique that is used in this paper for solving the inequality constraint problem is the slack-variable method. The slack-variable method converts the inequality constraint by introducing new variables γ_i satisfying the equations

$$(\Gamma_{max\,i} - \Gamma_i)(\Gamma_i - \Gamma_{min\,i}) = \gamma_i^2, \quad i = 1, 2, \ldots \quad (20)$$

It is easily demonstrated that Eq. (20) is equivalent to Eq. (19) since in order for $\gamma_i, i = 1, 2, \ldots$ to be real, Eq. (20) must be satisfied, and vice versa.
Function x is now said to be optimal if, in addition to the necessary conditions stated above, Eq. (20) is satisfied. It can be shown that this constrained problem is equivalent to the problem of maximizing the cost function

$$\mathbf{H}(\mathbf{x}(t), t) = \int_{t_o}^{t_f}\left[\mathbf{g}(\mathbf{x}(t), \dot{\mathbf{x}}(t), t) + \lambda_j(t)\left[(\Gamma_{max\,i} - \Gamma_i)(\Gamma_i - \Gamma_{min\,i}) - \gamma_i^2\right]\right] dt \quad (21)$$

Subject to no constraints, where the time-varying m-vector $\lambda(t)$ is the vector equivalent of the Lagrange multiplier [17].
We can summarize the two-point boundary-value problem that results from above-mentioned equations by the equations:

$$\dot{\mathbf{x}}^*(t) = \frac{\partial \mathbf{H}}{\partial \lambda} \quad (22)$$

$$\dot{\lambda}^*(t) = -\frac{\partial \mathbf{H}}{\partial \mathbf{x}} \quad (23)$$

With boundary conditions:

$$\mathbf{x}(t_\circ) = \mathbf{x}_\circ$$

$$\mathbf{x}(t_f) = \mathbf{x}_f$$

By knowing the boundary conditions, we could numerically integrate the differential equations to obtain optimal x. The numerical technique that has been used in this work is based on the following general procedure:

An initial guess is used to obtain the solution to a problem in which one or more of the necessary conditions stated before is not satisfied. The solution is then used to adjust the initial guess in an attempt to make the next solution come "closer" to satisfying all of the necessary conditions. If these steps are repeated and the iterative procedure converges, the necessary conditions will eventually be satisfied.

PROBLEM OF OPTIMIZATION OF INTAKE VALVE PROFILE IN ORDER TO MAXIMIZE VOLUMETRIC EFFICIENCY

In this section, we are seeking optimized intake valve profile and timing by using optimization techniques that have been described in last section. Therefore, we first form the cost function. Since the purpose is to maximize the volumetric efficiency we use the model that has been described in volumetric efficiency sub-section as cost function:

$$\mathbf{J}(\mathbf{x}) = \int_{t_\circ}^{t_f} \mathbf{g}(\mathbf{x}, \dot{\mathbf{x}}, t) \Rightarrow$$
$$\Rightarrow \eta_v\left(L_v(t), \theta_{IVO}(t), \theta_{IVC}(t)\right) = \int_{t_{IVO}}^{t_{IVC}} \frac{\dot{m}_{cyl}}{\rho V_d} dt \qquad (24)$$

With boundary condition:
$$t_\circ = t_{IVO} \Rightarrow L_v(t_\circ) = 0, \theta_{IVO}(t_\circ) = \theta_{IVO_\circ}, \theta_{IVC}(t_\circ) = \theta_{IVC_\circ}$$
$$t_f = t_{IVC} \Rightarrow L_v(t_f) = 0, \theta_{IVO}(t_f) = \theta_{IVO_f}, \theta_{IVC}(t_f) = \theta_{IVC_f}$$

INEQUALITY CONSTRAINT

As we have discussed before, we can characterize the camless valve motion by timing (or opening) IVO, maximum lift IVL, and closing IVC (IVO+IVD) of each intake valve. These are the parameters that varies with time which in order to find their optimal function we solve the necessary conditions of optimization problem described in last section for camless intake lift profile and intake valve timing.

There are three constraints in our problem that comprises maximum intake valve lift and limitations for value of intake valve opening and closing value that appears as inequality constraints in the form of following equations:

$$0 \leq L_v \leq L_{v\max} \Rightarrow \left(L_{v\max} - L_v\right)L_v - \alpha_1^{\,2} = 0 \qquad (25)$$

$$\theta_{IVO_{\min}} \leq \theta_{IVO} \leq \theta_{IVO_{\max}} \Rightarrow \left(\theta_{IVO_{\max}} - \theta_{IVO}\right)\left(\theta_{IVO} - \theta_{IVO_{\min}}\right) - \alpha_2^{\,2} = 0 \qquad (26)$$

$$\theta_{IVC_{\min}} \leq \theta_{IVC} \leq \theta_{IVC_{\max}} \Rightarrow \left(\theta_{IVC_{\max}} - \theta_{IVC}\right)\left(\theta_{IVC} - \theta_{IVC_{\min}}\right) - \alpha_3^{\,2} = 0 \qquad (27)$$

Thus the refined cost function will be in the form of:

$$\tilde{\eta}_v\left(L_v, \theta_{IVO}, \theta_{IVC}\right) =$$
$$\int_{t_{IVO}}^{t_{IVC}} \left[\frac{\dot{m}_{cyl}}{\rho v_d} + \lambda_1\left[\left(L_{v\max} - L_v\right)L_v - \alpha_1^{\,2}\right]\right]dt +$$
$$+ \int_{t_{IVO}}^{t_{IVC}} \lambda_2\left[\left(\theta_{IVO_{\max}} - \theta_{IVO}\right)\left(\theta_{IVO} - \theta_{IVO_{\min}}\right) - \alpha_2^{\,2}\right]dt +$$
$$+ \int_{t_{IVO}}^{t_{IVC}} \lambda_3\left[\left(\theta_{IVC_{\max}} - \theta_{IVC}\right)\left(\theta_{IVC} - \theta_{IVC_{\min}}\right) - \alpha_3^{\,2}\right]dt \qquad (28)$$

The specifications that have been used in optimization solution are as follows:
$$L_{v\max} = 3mm, \quad \theta_{IVO_{\min}} = 0, \quad \theta_{IVO_{\max}} = 20\deg,$$
$$\theta_{IVC_{\min}} = 180\deg, \quad \theta_{IVC_{\max}} = 220\deg$$

OPTIMIZED RESULTS

Applying optimization processes to model described in engine model section leads to nonlinear and coupled differential equations that had been coded in Matlab Simulink software. Furthermore, the Matlab stiff integration numerical algorithm was used to solve the nonlinear equations of the necessary conditions and boundary conditions of optimum system.

The optimization code run for maximized values of volumetric efficiency at different engine speeds and obtained results are compared with values of volumetric efficiency of conventional engine.

As it can be seen in Fig. 12, with optimization of intake valve lift profile and timing, volumetric efficiency has been improved in all engine speeds, especially at low engine speeds.

CONCLUSION

Variable valve timing (VVT) enables optimization for an engine's top-end performance, without compromising engine operation at low speeds and loads.

In the present work the performance of a camless unthrottled SI engine were analyzed with simulation of the phenomenological model of the engine breathing process of a SI engine. Although, the model of volumetric efficiency was simulated. This is in order to postulate optimal valve timing strategy for maximizing engine volumetric efficiency in terms of the intake valve lift profile.

Finally, we draw the following conclusions:

1   The breathing process of engine model simulated in this work agrees reasonably well with the analytical model [13].

2   A comparison of the volumetric efficiency model simulated in this work with experimental data from Ohata in [16] indicates that the model predicts the correct trend for volumetric efficiency at different engine speeds.

3   The numerical engine optimization, highlights the fact that camless optimized intake valve profile has the capability to increase the volumetric efficiency both at low and high speed conditions.

REFERENCES

[1] Ma, T.H. "Recent advances in Variable Valve Timing," Alternative and advanced Automotive Engines, Plenum Press, New York, 1996.

[2] Gray, C. "A Review of Variable Valve Timing," SAE Paper 880386, 1988.

[3] Elrod, A.C., and Nelson, M.T. "Development of a Variable Valve Timing Engine to Eliminate the Pumping Losses Associated with Throttled Operation," SAE Paper 860537, 1986.

[4] Anderson, M., and Levin, M. "Adaptive Lift Control for a Camless Electrohydraulic Valvetrain," SAE Paper 981029, 1998.

[5] Kim, D., Anderson, M., and Tsao, T.C. "A Dynamic Model of a Springless Electrohydraulic Camless Valvetrain System," SAE Paper 970248, 1997.

[6] Seilly, A.H. "Helenoid Actuators- A New Concept in Extremely Fast Acting Solenoids," SAE Paper 790119, 1979.

[7] Scott, D., "Variable Valve Timing to Boost Engine Efficiency," Popular Science, 1980.

[8] Ahmad, T., and Theobald, M.A. "A Survey of Variable Valve Actuation Technology," SAE Paper 891674, 1989.

[9] Sono, H., and Umiyama, H. "A Study of Combustion Stability of Non Throttling SI Engine with Early Intake Valve Closing Mechanism," SAE Paper 945009, 1994.

[10] Schecter, M.M., and Levin, M.B. "Camless engine," SAE Paper 960581, 1996.

[11] Ashhab, M.S., Stefanopoulou, A.G., Cook, J.A., and Levin, M. "Camless Engine Control for Robust Unthrottled Operation," SAE Paper 981031, 1998.

[12] Moraal, P.E., Cook, J.A., and Grizzle, J.W. "Modeling the Induction Process of an Automobile Engine," Control Problems in Industry, 1995, pp. 253-270.

[13] Miller, R.H., Davis, G.C., Newman, C.E., and Levin, M.B. "Unthrottled camless valvetrain strategy for spark-ignited Engines," Proceedings of the 19th Annual Fall Technical Conference of the ASME Internal Combustion Engine Design Division, Advanced Engine Design, ed. T. Uzkan, ICE-Vol.29-1, 1997, pp.81-94.

[14] Heywood, J. B. Internal Combustion Engine Fundamentals, McGraw-Hill, New York, NY, 1988.

[15] Ashhab, M.S., Stefanopoulou, A.G., Cook, J.A., and Levin, M. "Control-Oriented Model for Camless Intake Process-Part 1," ASME Journal of Dynamic Systems, Measurement, and Control, 2000, 122:122-130.

[16] Ohata, A., and Ishida, Y. "Dynamic Inlet Pressure and Volumetric Efficiency of Four Cylinder Engine," SAE Paper 820407, 1982.

[17] Sage, A. P. Optimum Systems Control, Prentice-Hall, New Jersey, NJ.
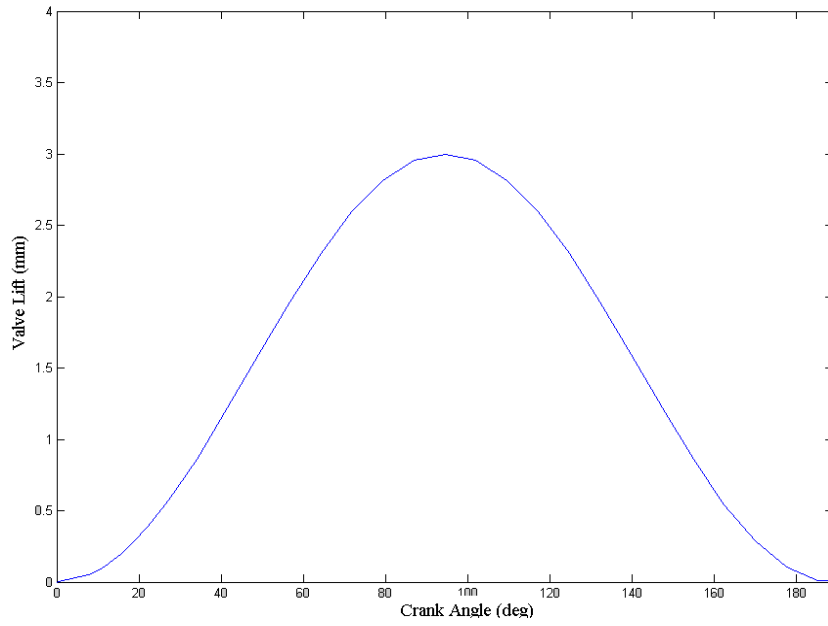
Fig.1 Conventional intake valve profile
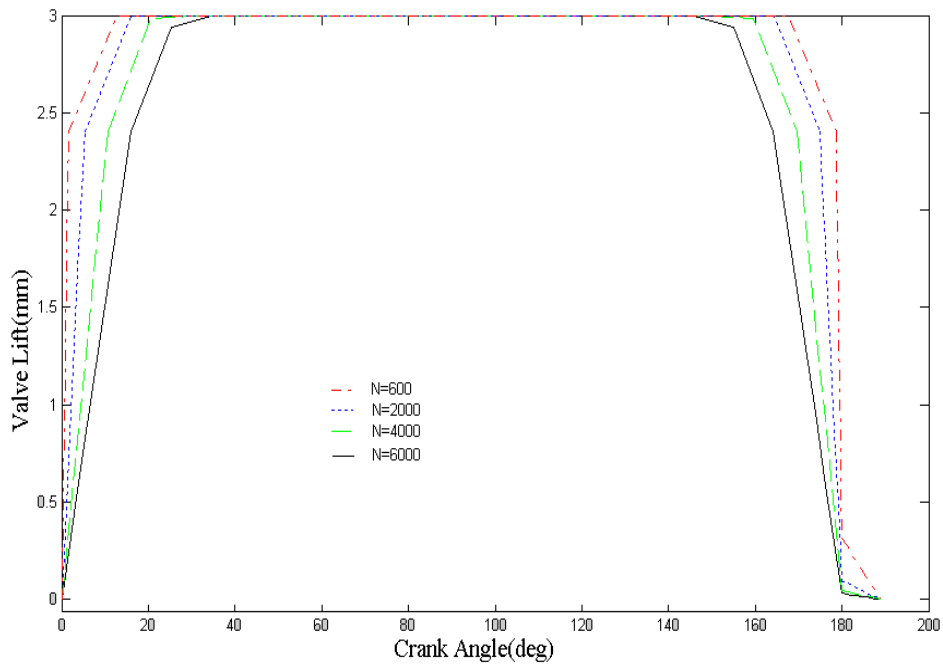
Fig.2 Camless intake valve profiles for different engine speeds
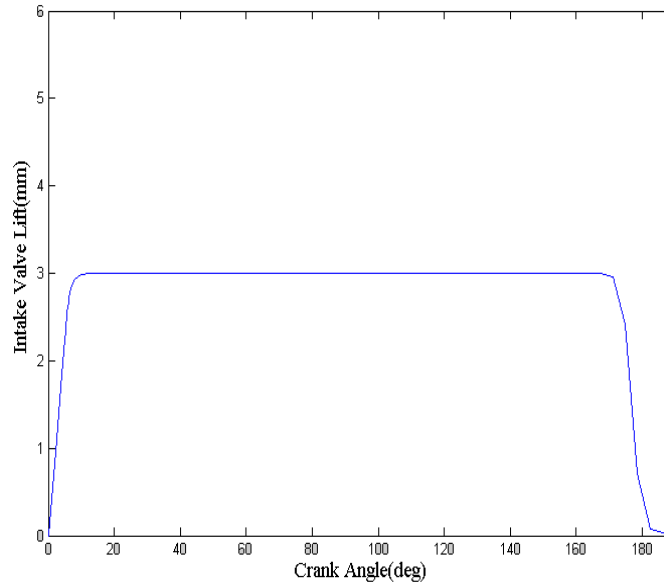
Fig.3 Camless intake valve profile at an engine speed of 2000 rpm
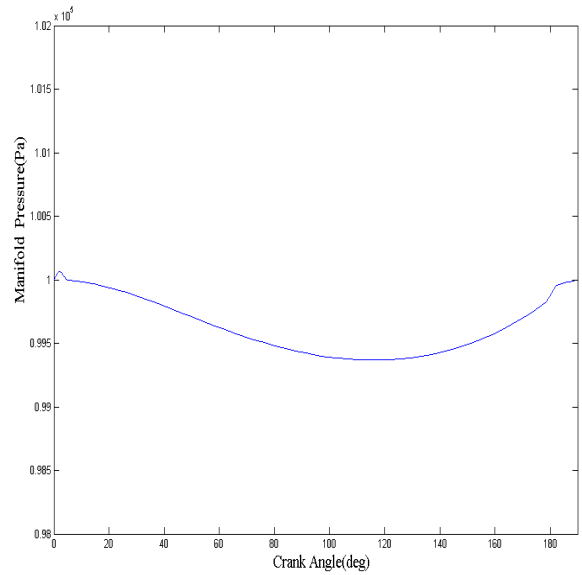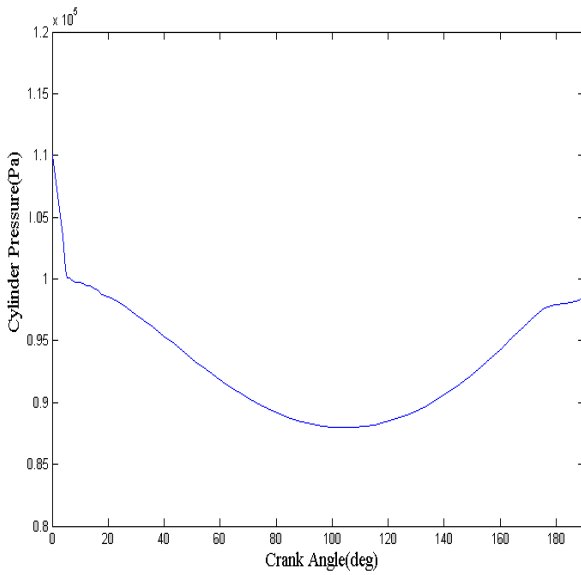
Fig.4 Cylinder and manifold pressures of a 4-cylinder engine at an engine speed of 2000 rpm
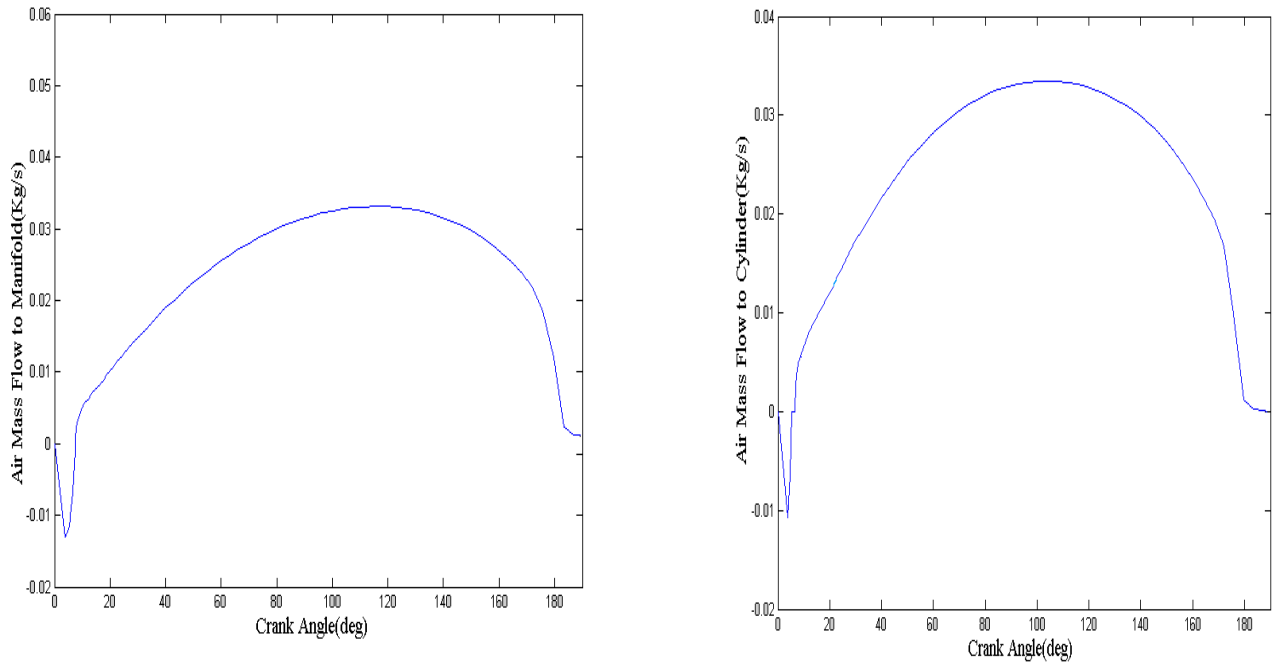
Fig.5 Air mass flow to manifold and cylinder of a 4-cylinder engine at an engine speed of 2000 rpm
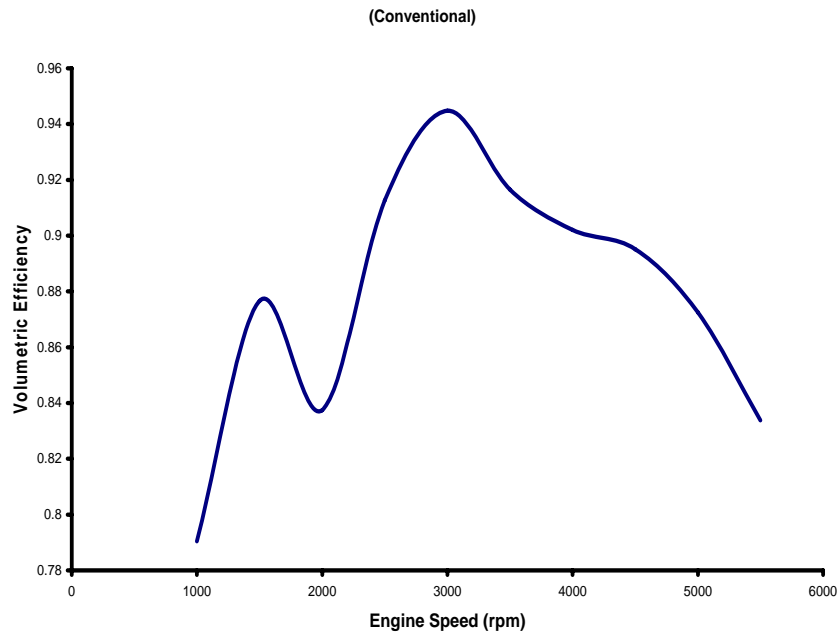
(Conventional)

Fig.6 Volumetric efficiency of a conventional 4-cylinder engine at different engine speeds
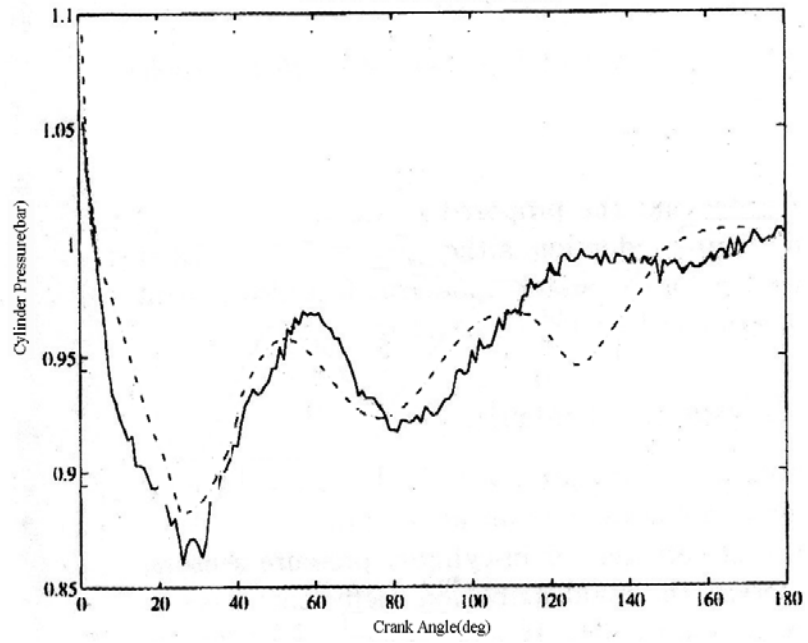
Fig. 7   Cylinder pressure experimental data (solid line) and Simulation Results (dashed line) at 1500 rpm
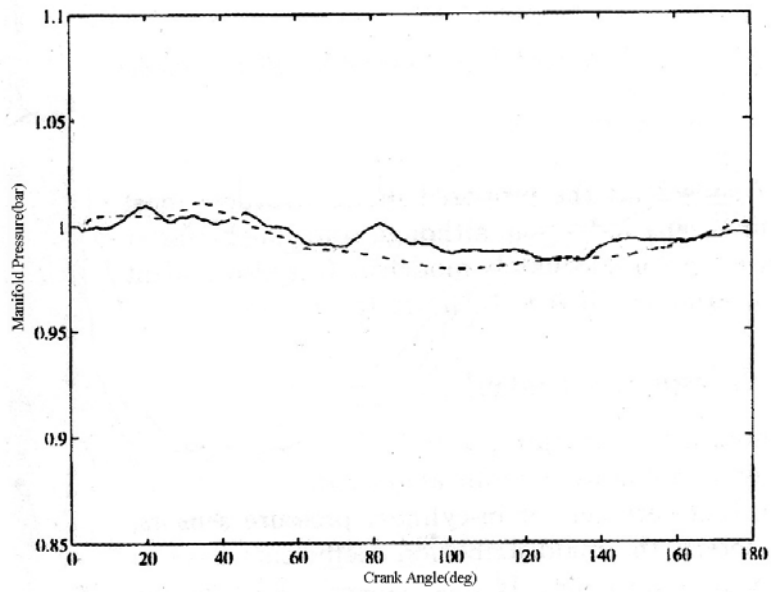
Fig .8 Manifold pressure experimental data (solid line) and Simulation Results (dashed line) at 1500 rpm
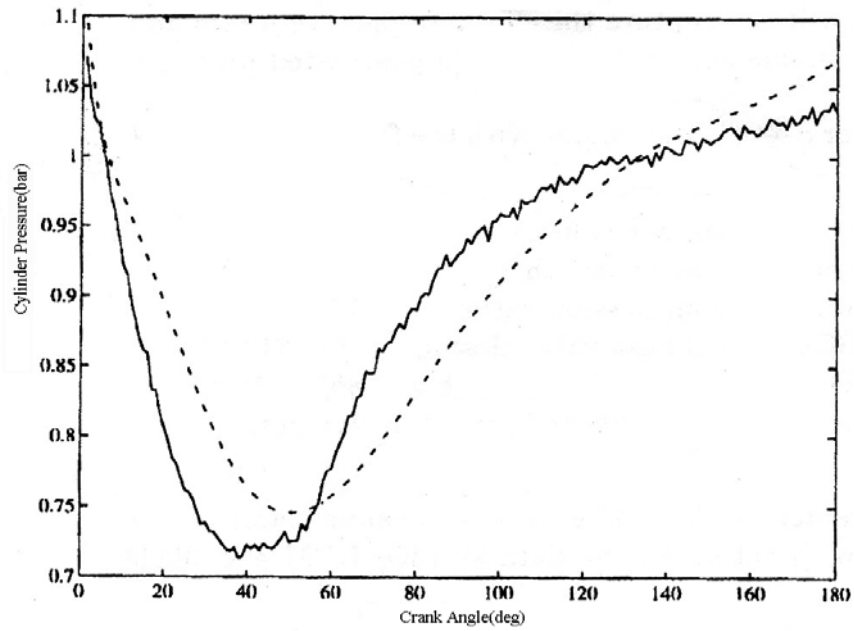
Fig .9 Cylinder Pressure experimental data (solid line) and Simulation Results (dashed line) at 3000 rpm
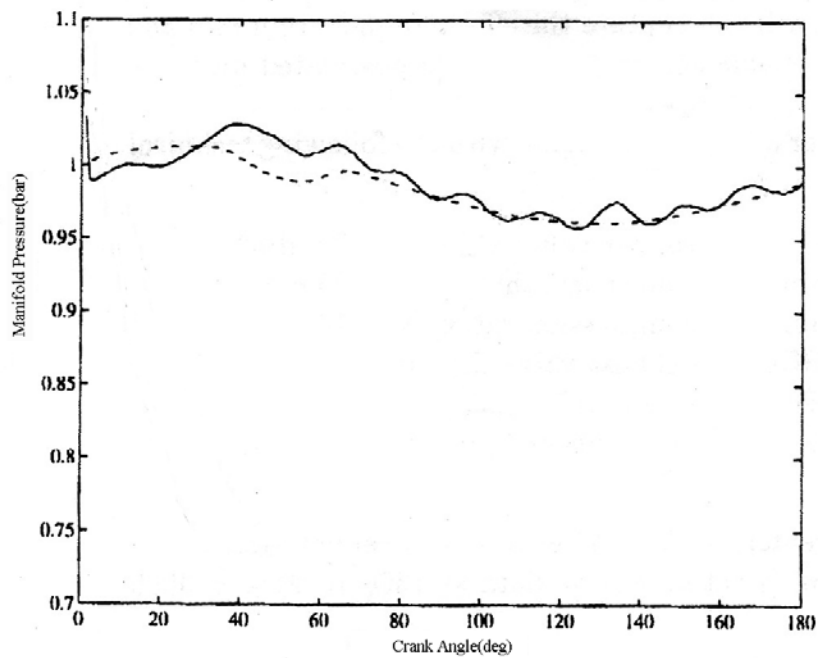
Fig .10 Manifold pressure experimental data (solid line) and Simulation Results (dashed line) at 3000 rpm
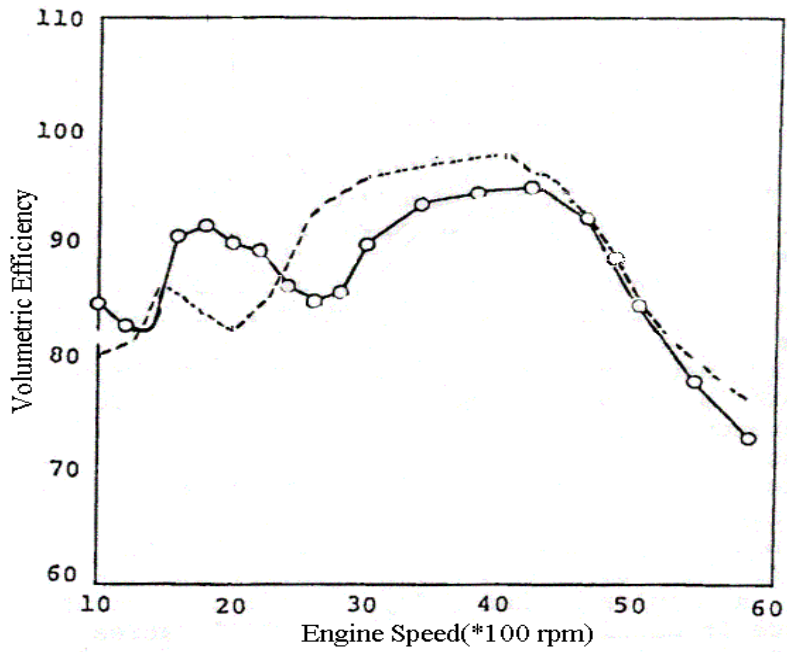
Fig .11 Volumetric efficiency experimental data (solid line with circles) and Simulation Results (dashed line) at different engine speeds
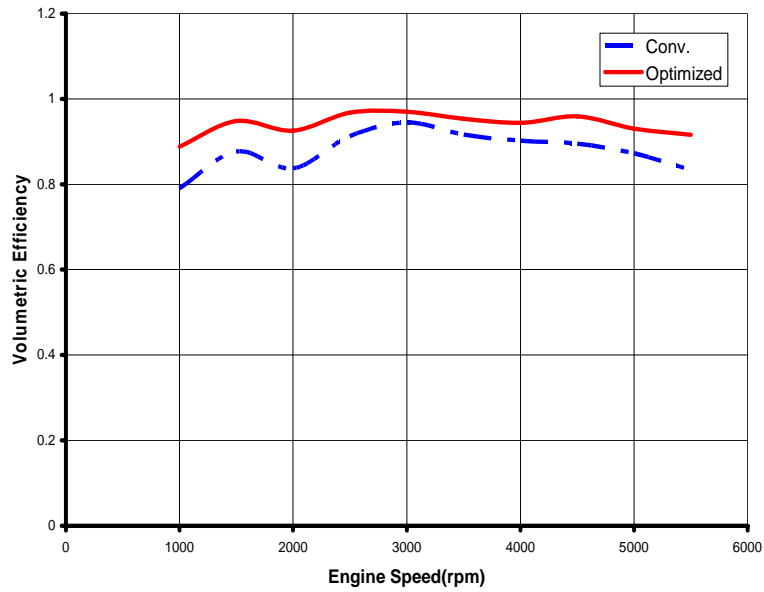
Fig.12 Volumetric efficiency optimized (red line) and conventional (blue line) at different engine speeds

15   Copyright © 2006 by ASME